#56

J. Phys. Chem. Solids Vol. 42, pp. 143–151
Pergamon Press Ltd., 1981. Printed in Great Britain

Papers from the GEOPHYSICAL LABORATORY
Carnegie Institution of Washington
No. 1830

0022-3697/81/030143-09$02.00/0

BULK MODULI AND HIGH-PRESSURE CRYSTAL STRUCTURES OF RUTILE-TYPE COMPOUNDS

ROBERT M. HAZEN and LARRY W. FINGER
Geophysical Laboratory, Carnegie Institution of Washington, Washington, DC 20008, U.S.A.

(*Received* 27 *February* 1980; *accepted* 9 *June* 1980)

Abstract—Unit-cell parameters and crystal structures of five rutile-type compounds, including TiO_2, SnO_2, GeO_2, RuO_2 and MnF_2, have been determined at pressures to 50 kbar at 20°C. All five compounds compress anisotropically with the *a* axis approximately twice as compressible as *c*. The one variable positional parameter, *x* of oxygen or fluorine, changes little with pressure.

The uniform behavior of these RX_2 compounds at high pressure contrasts with their highly variable structural changes at high-temperature. Rutile-type oxides are, therefore, unlike most oxides and silicates, in which structural variations at high pressure mirror those at high temperature.

INTRODUCTION

The rutile structure is the most common form for RX_2 compounds in oxides and fluorides. Common minerals with this structure, in addition to TiO_2, include cassiterite (SnO_2), pyrolusite (MnO_2), and plattnerite (PbO_2). Furthermore, the rutile form of SiO_2, stishovite, is stable at pressures greater than 80 kbar. This structure may thus play a significant role in mantle mineralogy.

The high-pressure behavior of rutile-type oxides and fluorides has been studied extensively by geophysicists interested in mantle processes. Investigations of the elastic properties and phase transitions of difluorides (MnF_2, NiF_2, MgF_2 and FeF_2) have demonstrated a complex variety of transformation behavior at moderate pressure[1, 2]. Dioxides of the rutile form have also been the subject of high-pressure studies that yield additional data on their elastic constants[3] and phase transitions[4].

Rutile is tetragonal with space group $P4_1/nmm$ and $z = 2$. A basic building block of the structure is the RX_6 octahedron; edge-linked chains of octahedra extend parallel to the *c* axis. Each chain is linked to four others by a corner sharing of anions. Two symmetrically distinct atoms in each unit cell are the octahedrally coordinated *R* at (0, 0, 0) and the anion *X* at (*x*, *x*, 0) with $x = 0.3$.

The crystal chemistry of rutile-type compounds has been investigated and reviewed by Baur and Khan[5], who cite earlier literature. The high-temperature crystal structure of TiO_2 reported by Meagher and Lager[6] and the high-pressure structure of MnF_2 determined by Hazen *et al.*[7] are the only previously reported single-crystal structures of rutile-type compounds under non-ambient conditions. The present study of the high-pressure structural variation of several RX_2 compounds was undertaken in order to evaluate empirical bond compression relationships and to predict high-pressure structures of other rutile isomorphs.

EXPERIMENTAL

Specimen description

Specimens of synthetic TiO_2 and SnO_2 were kindly provided from the collections of the Smithsonian Institution (USNM 136751 and 136749, respectively) by John S. White. The rutile was prepared from a sodium borate flux under slow cooling by John S. Berkes, Pennsylvania State University, and the cassiterite was grown by vapor transport (1650–1400°C gradient) in an argon flux from an oxide powder by J. P. Fillard, Universite du Languedoc, Academie de Montpellier, France.

Ruthenium dioxide was generously provided by S. La Placa, IBM Watson Research Laboratory, from material synthesized by Shafer *et al.*[8]. Crystals were grown by the transport and oxidation of ruthenium metal. A single crystal of rutile-type GeO_2 was supplied by J. Mammone, Geophysical Laboratory, from commercially synthesized material.

T. Yagi provided crystals of MnF_2 from the synthetic material of K. Kohn, who dissolved metallic manganese in dilute hydrofluoric acid and then crystallized the solution by evaporation.

Data collection at room pressure

Data from the five rutile-type compounds were collected on crystals 60–100 μm in maximum diameter. The RuO_2 sample was a polished sphere 60 μm in diameter, and all other crystals were rectangular cleavage fragments. The intensities of all reflections in one quadrant with $(\sin\theta)/\lambda < 0.7$ were measured by a Picker, automated, four-circle diffractometer system with Nb-filtered MoK_α radiation[9]. Lattice parameters were refined from diffractometer angles of at least 12 centered reflections. Intensities were measured by a constant-precision procedure in which the background counting time and scan rate were dynamically adjusted so that the ratio of the intensity to the standard deviation calculated from counting statistics was of the order of 100[9].

High-pressure techniques

Flat cleavage plates approximately $100 \times 100 \times 30$ μm were used in high-pressure experiments on TiO_2, SnO_2, GeO_2 and MnF_2. The polished sphere was used for RuO_2 experiments. Crystals were mounted in a miniature cell with opposed diamond anvils designed by Merrill and Bassett[10] as modified by Hazen and Finger[11]. Inconel 750X gaskets (International Nickel Company, Inc.) and 4:1 methanol:ethanol as the hydrostatic pressure fluid were used. Ruby crystals were included in the

mount for pressure calibration by the shift in R_1 fluorescence wavelength[12]. Details of high-pressure procedures for crystal mounting and crystal centering are given elsewhere[11, 13].

Data collection and refinement

Lattice constants of crystals at high pressure were determined with 12–20 reflections, corrected for errors in crystal centering and diffractometer alignment by the method of Hamilton[14], as modified by King and Finger[15]. The apparent position of the diffracted radiation for each reflection was measured in eight different settings, four at positive and four at negative 2θ. Each set of data was refined without constraint, and the resulting "triclinic" cell was checked for agreement with the tetragonal symmetry of rutile-type compounds. These symmetry conditions are satisfied within two standard deviations for all five compounds at all pressures studied (Table 1). It is assumed, therefore, that conditions were hydrostatic and that no deviations from tetragonal dimensionality occurred.

Intensity data were collected for all accessible reflections with $(\sin\theta)/\lambda < 0.7$. The fixed-$\phi$ mode of data collection was used to maximize reflection accessibility and minimize attenuation by the diamond cell[16], and a correction was made for X-ray absorption by the diamond and beryllium components of the pressure cell as described by Finger and Hazen[17].

All intensity data were corrected for absorption by the crystal, and a parameter required for secondary extinction calculations[18] was computed. For each data set the average structure factor was calculated for reflections related by symmetry. No systematic deviations from ideal tetragonal symmetry were observed.

Least-squares refinement of the structural parameters was performed by program RFINE[19] with neutral scattering factors from Cromer and Mann[20] and the anomalous scattering coefficients of Cromer and Libermann[21]. Isotropic temperature factors and an isotropic correction for secondary extinction were used in each refinement. In the final cycles of refinement of SnO_2 and GeO_2 the extinction factor was fixed owing to very high (>98%) correlation between extinction and the metal temperature factor. The temperature factors for MnF_2, TiO_2 and SnO_2 were converted to anisotropic form for room-pressure data sets. The metal cations vibrate isotropically, but the anion vibration ellipsoids approximate prolate spheroids with axis of maximum vibration in the (001) plane, perpendicular to cation–anion bonds in that plane. Refinement conditions and refined isotropic structural parameters are given in Table 2.

RESULTS

Linear compressibilities and bulk moduli

Linear compressibilities and bulk moduli have been calculated from unit-cell data in Table 1. Unit-cell edges a and c may be expressed as functions of pressure:

$$a = a_0 + d_1P + d_2P^2. \quad (1)$$

A single d_1 term is sufficient to characterize linear compression in four of the five rutile-type compounds, but in TiO_2 the d_2 coefficients for a and c are nonzero. Coefficients of linear compressibility ($\beta_l = \Delta l/l\Delta p$) parallel to c ($\beta_\parallel$) and perpendicular to c ($\beta_\perp$) are recorded in Table 3 with values of a_0, c_0, d_1 and d_2 for each axial direction. In all five materials the a axis is more than twice as compressible as c. This anisotropy is perhaps due to metal–metal repulsion parallel to c across the shared octahedral edge. Linear compressibilities of MnF_2 to 15 kbar are approximately three times those of oxide isomorphs, because of weaker bonding in the fluoride.

Bulk moduli were calculated from unit-cell volume vs pressure data, using least-squares procedures. Estimated errors on the bulk moduli are based on errors in cell volumes and pressure measurements. Bulk moduli for TiO_2, SnO_2 and GeO_2 are 2.16(2), 2.18(2) and 2.58(5) Mbar, respectively. It is assumed that $K' = 7$[22, 23], and a first-order Birch–Murnaghan equation of state is used. These values are in agreement within ±10% of the values recorded by Liebermann[3], who used ultrasonic measurements on hot-pressed polycrystalline aggregates. Ming and Manghnani[24] measured the isothermal compression of TiO_2 to 100 kbar using powder X-ray diffraction and obtained $K_0 = 2.11 \pm 0.07$ Mbar ($K' = 6.8$), which is consistent with this study. The bulk modulus of MnF_2 was determined to be 0.94(3) Mbar, in close agreement with the results of Manghnani and Jamieson[25], who used single-crystal ultrasonic techniques. Thus, data from powder and single-crystal X-ray experiments at high pressure, as well as from ultrasonic studies, yield similar elastic constants.

Transition of MnF_2 to the α-PbO_2 structure

The single crystal of MnF_2 was observed in the diamond cell to transform from a square (011) plate to a diamond-shaped plate at pressures between 15 and 17 kbar. The formerly right angles were approx. 75 and 105° after the transition. Although a single crystal was preserved, diffraction maxima were broad and in some places split, and optical extinction was irregular, indicating severe strain and possible twinning of the high-pressure phase.

Twelve moderate to strong diffuse reflections from this new phase of MnF_2 were measured and yielded an orthorhombic unit cell: $a = 4.935(1)$, $b = 5.629(8)$, $c = 5.469(12)$, A, $\alpha = \beta = \gamma = 90.0(1)°$ and $V = 151.9(4)$ A^3. This 17-kbar unit cell and the associated intensities correspond closely to those of the α-PbO_2 structure. A transition of polycrystalline MnF_2 from rutile to α-PbO_2 structure was observed by Manghnani and Jamieson[25] to occur at 13 kbar. It is likely that the single crystal transforms at a slightly higher pressure owing to resistance inherent in the shear transformation.

High-pressure crystal structures

Refined structural parameters for rutile-type compounds at room and high pressures are recorded in Table 2. Two variable parameters, unit-cell c/a and the oxygen x fractional coordinate, are sufficient to define the rutile

Table 1. Unit-cell dimensions*

Specimen	Pressure (kbar)	a_1 (Å)	a_2 (Å)	c (Å)	α_1 (°)	α_2 (°)	γ (°)	V (Å^3)	c/a
TiO_2	0.001	4.5931(2)†	4.5928(2)	2.95837(8)	89.999(3)	90.003(3)	89.997(4)	62.408(4)	0.64411(4)
	15.5(5)	4.5811(4)	4.5803(4)	2.95461(8)	89.991(5)	90.008(5)	90.008(6)	61.995(7)	0.64501(7)
	27.5(5)	4.5706(4)	4.5707(4)	2.95126(8)	90.004(6)	89.994(5)	90.009(7)	61.653(8)	0.64570(7)
	37.0(5)	4.5623(5)	4.5630(7)	2.9489(2)	90.002(8)	90.001(7)	90.007(10)	61.389(12)	0.6463(1)
	48.4(5)	4.5547(3)	4.5547(2)	2.94661(6)	90.006(4)	90.000(4)	90.003(4)	61.129(5)	0.64694(4)
SnO_2	0.001	4.7373(1)	4.7368(2)	3.1862(1)	89.999(3)	90.003(3)	90.002(3)	71.496(4)	0.67261(4)
	18.0(5)	4.7207(3)	4.7211(1)	3.1818(1)	90.004(3)	89.991(5)	90.000(4)	70.912(6)	0.67398(5)
	41.6(5)	4.7032(5)	4.7033(2)	3.1759(3)	90.003(5)	89.999(8)	90.000(6)	70.252(10	0.67526(8)
	49.6(5)	4.6960(1)	4.6961(3)	3.1736(3)	90.004(7)	90.008(5)	90.000(4)	69.987(8)	0.67580(7)
GeO_2	0.001	4.3965(1)	4.3963(1)	2.8626(1)	90.006(3)	89.997(3)	90.001(2)	55.330(3)	0.65112(5)
	17.1(5)	4.3854(2)	4.3858(3)	2.8598(3)	89.990(7)	90.000(7)	90.000(4)	55.005(7)	0.65209(7)
	31.9(5)	4.3750(1)	4.3754(2)	2.8574(3)	89.999(6)	89.992(5)	89.994(3)	54.696(6)	0.65309(6)
	37.0(5)	4.3712(2)	4.3710(2)	2.8558(3)	89.99(7)	89.997(7)	90.011(4)	54.565(7)	0.65334(7)
MnF_2	0.001	4.8726(11)	4.8735(11)	3.3101(9)	90.04(2)	90.02(2)	90.00(1)	78.60(3)	0.6793(2)
	10(1)	4.8495(13)	4.8513(12)	3.3043(13)	89.99(1)	90.01(3)	89.99(1)	77.74(4)	0.6812(2)
	15(1)	4.8411(2)	4.8416(2)	3.3002(5)	89.98(1)	90.02(1)	89.99(1)	77.35(1)	0.6817(1)
RuO_2	0.001	4.4906(2)	4.4904(2)	3.1065(2)	89.998(4)	89.992(4)	90.007(4)	62.640(5)	0.6918(1)
	11.1(5)	4.4839(5)	4.4837(1)	3.1044(3)	90.005(5)	90.004(8)	89.991(7)	62.412(9)	0.6924(1)
	27.9(5)	4.4721(11)	4.4717(12)	3.100(2)	90.00(3)	89.98(3)	90.00(2)	61.99(4)	0.6932(4)
	28.3(5)	4.4704(6)	4.4715(6)	3.1020(8)	90.00(2)	90.00(2)	90.02(2)	62.01(2)	0.6938(1)

*Cell parameters, refined from at least 96 centered reflections (8 positions of at least 12 hkl's), are treated as triclinic to detect deviations from tetragonal dimensionality. All materials are consistent with tetragonal symmetry within 2 esd.

†Parenthesized figures represent esd's of least units cited.

Table 2. Refinement conditions and refined parameters

Specimen	μ_ℓ (cm^{-1})	Pressure (kbar)	Crystal Number	Weighted R(%)	R (%)	Number of Observations	X_O	B_M	B_O	r^* ($\times 10^5$)
TiO_2	61.2	0.001	1	2.2	2.0	98	0.3051(3)†	0.52(2)	0.46(3)	1.1(1)
		15.5(5)	2	3.9	4.3	43	0.3042(13)	0.46(7)	0.58(13)	0.7(2)
		27.5(5)	2	4.1	4.0	44	0.3063(12)	0.44(6)	0.49(11)	0.6(2)
		37.0(5)	2	2.9	4.2	57	0.3027(7)	0.40(4)	0.32(8)	0.4(1)
		48.4(5)	2	4.8	5.2	36	0.3078(16)	0.54(10)	0.64(15)	1.0(5)
SnO_2	173.6	0.001	1	1.2	1.7	99	0.3064(4)	0.27(1)	0.48(4)	1.17(7)
		18.0(5)	2	3.5	3.0	61	0.3064(22)	0.31(3)	0.41(18)	8.1‡
		41.6(5)	2	3.8	3.1	60	0.3096(23)	0.35(3)	0.57(23)	6.3‡
		49.6(5)	2	3.9	3.7	45	0.3105(23)	0.40(4)	0.27(22)	9.7‡
GeO_2	265.6	0.001	1	5.3	4.5	88	0.3061(13)	0.30(6)	0.45(11)	17.9(26)
		17.1(5)	1	4.1	4.3	39	0.3060(26)	0.45(6)	0.4(3)	17.9‡
		31.9(5)	1	3.5	4.0	39	0.3047(20)	0.43(5)	0.4(2)	17.9‡
		37.0(5)	1	5.8	5.9	31	0.3035(43)	0.57(11)	0.3(4)	17.9‡
MnF_2	76.5	0.001	1	1.5	1.4	179	0.30496(13)	0.65(1)	1.08(1)	0.98(8)
		10(1)	1	1.2	1.3	32	0.3046(3)	0.74(9)	1.89(26)	0.6(3)
		15(1)	1	1.5	1.6	28	0.3046(5)	0.77(12)	1.62(26)	0.3(4)
RuO_2	116.7	0.001	1	1.4	1.5	97	0.3057(4)	0.22(1)	0.40	0.24(1)
		11.1(5)	1	2.5	2.3	59	0.3064(12)	0.39(3)	0.57	0.27(3)

†Parenthesized figures represent esd's of least units cited.

‡r^* held constant in last cycles due to high correlation (>0.98) between r^* and isotropic temperature parameters.

Table 3. Linear compressibilities and bulk moduli

Compound	Axis	ℓ_0 (Å)	b_1 ($\times 10^4$ kbar^{-1})	b_2 ($\times 10^7$ kbar^{-2})	β_ℓ ($\times 10^4$ kbar^{-1})	$\beta\perp/\beta_{//}$	K_0 (Mbar) [K']
TiO_2	a	4.5930(1)	8.3(3)	9(3)	1.8	2.0	2.22(2) [4] 2.16(2) [7]
	c	2.9584(1)	2.7(2)	5(4)	0.9		2.20(9) [5(4)]
SnO_2	a	4.737(1)	8.2(2)	—	1.73	2.2	2.24(2) [4]
	c	3.1862(1)	2.50(4)	—	0.78		2.18(2) [7]
GeO_2	a	4.3965(3)	6.7(1)	—	1.52	2.6	2.65(5) [4]
	c	2.8626(1)	1.7(1)	—	0.59		2.58(5) [7]
RuO_2	a	4.4906(3)	6.7(3)	—	1.5	2.6	2.70(6) [4]
	c	3.1065(2)	1.8(2)	—	0.6		
MnF_2	a	4.872(1)	20.8(9)	—	4.3	2.2	0.94(3) [4]
	c	3.3102(5)	6.6(4)	—	2.0		

structure. In all five rutile-type compounds c/a increases significantly with pressure because of the greater compressibility of a. The oxygen x coordinate does not vary systematically with pressure in TiO_2, RuO_2 or MnF_2. The parameter may increase slightly in SnO_2 and decrease slightly in GeO_2 with pressure, but in no case is the variation greater than two standard deviations.

In terms of octahedral subunits, details of the rutile structure are little altered over the pressure ranges studied. Interoctahedral cation–anion–cation angles and intraoctahedral anion–cation–anion angles (Table 4) change by only a few tenths of a degree, and distortion indices are similarly constant, in TiO_2, RuO_2 and MnF_2. Octahedra in these three compounds compress slightly, scaling in the same way as the unit cell. Polyhedral distortions increase in SnO_2 and decrease in GeO_2 with pressure owing to the small changes in oxygen parameter x, but these changes are small compared with experimental errors.

Polyhedral bulk moduli

Polyhedral bulk moduli, K_p, calculated from polyhedral volume data in Table 4 are (in Mbar) 2.2(8), 1.8(8), 2.7(8), 2.2(12) and 1.0(3) for octahedra of Ti, Sn, Ge, Ru and Mn, respectively. These values are all within one estimated standard deviation of bulk moduli, K_0, as expected from the relatively small distortions of octahedra with pressure.

Hazen and Finger[26] proposed a simple bulk modulus-volume relationship for predicting polyhedral bulk moduli in compounds:

$$K_p = \frac{7.5\, S^2\, Z_c Z_a}{\langle d \rangle^3},$$

where z_c and z_a are cation and anion formal charge, $\langle d \rangle$ is the mean cation–anion bond distance, and S^2 is an empirical ionicity term equal to 0.50 for oxides and 0.75 for fluorides. This equation, with bond distances in Table 4, may be used to calculate octahedral bulk moduli of 4.0, 4.9, 4.6, 5.5 and 1.3 for Ti, Sn, Ge, Ru and Mn, respectively. All predicted values for oxides are greater than observed by as much as a factor of two, though the Mn–F octahedral predicted bulk modulus lies within the limits of observational error. The failure of the Hazen and Finger bulk modulus-volume relationship to model $R^{4+}O^{2-}$ octahedral compression is perhaps due to the greater covalency (i.e. smaller S^2) of these bonds[27, 28] compared with R^{2+} octahedra from which the relationship was largely derived. These discrepancies notwithstanding, the predicted and calculated bulk moduli for octahedra in rutile-type oxides are among the largest yet observed in any compounds.

Comparison of high-temperature and high-pressure structures

Structural parameters in many ionic compounds are primarily a function of molar volume. In these materials structural variation with increasing pressure or decreasing temperature (both of which decrease molar volume) are similar, as illustrated in Fig. 1(a). This "inverse relationship" between the temperature and pressure response of solids is qualitatively, if not quantitatively, true for many minerals[29–32]. Until this study, all materials for which both high-temperature and high-pressure structures have been reported demonstrated qualitative agreement with the inverse relationship.

Rao[33] reported linear thermal expansion coefficients for 13 fluorides and oxides of the rutile type. In sharp contrast to their uniformity of compression, these materials show a wide variation in thermal expansion anisotropy. The ratio of expansion coefficients parallel and perpendicular to c varies from -2.5 in RuO_2, to 0.4 in MnF_2, to 0.9 in SnO_2 and to 2.1 in GeO_2. The c-axis expansion is negative in some rutile-type compounds, but in others it is positive and greater than expansion of the a axis. The complex behavior of these isostructural compounds was attributed by Rao to varying degrees of bond ionicity and nonspherical electron effects. The great variation in the high-temperature behavior of the rutile isomorphs is evidence that the inverse relationship does not apply to these compounds.

The only report on a rutile structure at high temperature is the study by Meagher and Lager[6] on TiO_2. The oxygen x parameter does not vary with temperature or with pressure. With increasing temperature, however, c/a increases, a result which is the opposite of the trend predicted by the inverse relationship (Fig. 1b). A similar anomaly is observed in the shift of Raman modes. Samara and Peercy[34] measured TiO_2 Ramam spectra at both high temperature and high pressure and recorded violations of the opposite shift of these modes that is usually observed. This behavior implies that structural and physical parameters in rutile are not controlled by molar volume, as they are in many other ionic compounds.

Baur and Khan[5] summarized the crystal chemistry of twenty rutile isomorphs and concluded that nonspherical electron configurations of the metal ions play a dominant role in determining octahedral distortions. Furthermore, the ratio of c and a axes was observed to be lower in those rutile-type compounds with strong metal–metal interactions. A third influence on the structural details of these isomorphs is the degree of covalent bonding. By implication, one or more of these effects—nonspherical electrons, metal–metal interactions, or bonding covalency—vary significantly, but not inversely, with changes in temperature and pressure.

CONCLUSIONS

Rutile isomorphs do not conform to the inverse relationship that has been observed in most other oxides and silicates studied to date. Why should some materials have structures dependent on molar volume, whereas others do not? The answer may lie in the relative influence of electrostatic forces vs covalency and nonspherical electron distribution. The former are dependent on atomic positions but independent of temperature and pressure. The latter vary with temperature and pressure. In the majority of compounds for which the inverse relationship has been demonstrated (e.g. feldspars,

Table 4. Selected interatomic distances and angles, octahedral volumes, and distortion indices

Specimen	Pressure (kbar)	M-X_1 [4]*	M-X_2 [2]	X_1-X_1 [2]	X_1-X_2 [8]	X_2-X_2 [2] ≡ M-M	X-M-X	M-X-M	Octa. Vol. (A^3)	Quad.‡ Elon.	Angle‡ Vari.
TiO_2	0.001	1.947(1)†	1.982(2)	2.532(4)	2.778(1)	2.9584(1)	81.1(1)	130.6(1)	9.90	1.008	28.7
	15.5(5)	1.947(1)	1.971(9)	2.536(17)	2.770(2)	2.9546(1)	81.3(4)	130.6(2)	9.81	1.009	31.6
	27.5(5)	1.935(5)	1.980(8)	2.503(16)	2.769(2)	2.9513(1)	80.6(4)	130.3(2)	9.79	1.008	28.0
	37.0(5)	1.948(3)	1.953(5)	2.546(10)	2.759(1)	2.9489(2)	81.6(2)	130.8(1)	9.78	1.007	25.6
	48.4(5)	1.924(7)	1.983(10)	2.476(21)	2.763(3)	2.9466(1)	80.1(5)	130.0(2)	9.64	1.010	35.8
SnO_2	0.001	2.054(2)	2.053(3)	2.594(6)	2.904(1)	3.1862(1)	78.3(1)	129.2(1)	11.31	1.014	49.8
	18.0(5)	2.050(9)	2.046(14)	2.585(29)	2.896(3)	3.1818(1)	78.2(6)	129.1(3)	11.22	1.014	50.9
	41.6(5)	2.031(10)	2.059(16)	2.533(31)	2.892(4)	3.1759(3)	77.2(2)	128.6(3)	11.04	1.017	60.1
	49.6(5)	2.025(10)	2.062(15)	2.516(31)	2.890(4)	3.1736(3)	76.8(7)	128.4(3)	10.98	1.018	63.2
GeO_2	0.001	1.871(5)	1.903(8)	2.411(16)	2.669(2)	2.8626(1)	80.2(4)	130.1(2)	8.76	1.010	34.8
	17.1(5)	1.869(10)	1.898(16)	2.41(3)	2.663(4)	2.8598(3)	80.2(8)	130.1(4)	8.71	1.010	35.2
	31.9(5)	1.871(8)	1.886(12)	2.42(3)	2.656(3)	2.8574(3)	80.4(6)	130.2(3)	8.68	1.009	33.2
	37.9(5)	1.874(17)	1.875(17)	2.43(5)	2.652(7)	2.8558(3)	80.8(12)	130.4(6)	8.68	1.009	30.9
MnF_2	0.001	2.132(1)	2.102(1)	2.688(2)	2.994(1)	3.3101(9)	78.2(1)	129.1(1)	12.47	1.015	51.0
	10(1)	2.127(2)	2.089(2)	2.680(4)	2.982(1)	3.3043(13)	78.1(1)	129.0(1)	12.34	1.015	51.4
	15(1)	2.124(2)	2.086(3)	2.676(6)	2.977(1)	3.3002(5)	78.1(1)	129.0(1)	12.28	1.015	51.8
RuO_2	0.001	1.984(2)	1.941(2)	2.468(5)	2.7756(6)	3.1065(3)	76.9(1)	128.5(1)	9.92	1.018	62.1
	11.1(5)	1.979(6)	1.943(9)	2.455(12)	2.773(6)	3.1044(3)	76.7(2)	128.4(2)	9.87	1.019	64.5

*Bracketed figures represent bond multiplicity.

†Parenthesized figures represent *esd*'s of least units cited.

‡Quadratic elongation and bond angle variance are distortion parameters defined by Robinson *et al.*[36]. Values for regular polyhedra are 1.0 and 0.0 respectively.

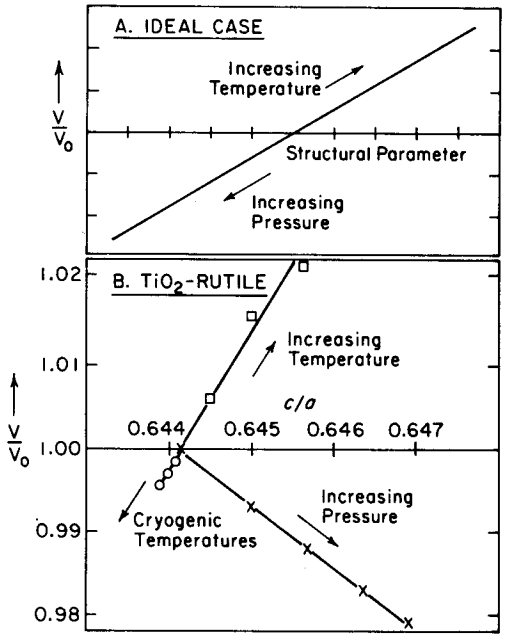

Fig. 1. The inverse relationship between structural changes with temperature and pressure. (a) The ideal case, in which structural parameters are functions of molar volume (expressed as V/V_0). Temperature changes of structure are thus the opposite of pressure changes. Most oxides and silicates conform to this inverse relationship. (b) Rutile c/a increases both with temperature and pressure, thus violating the inverse relationship. High-temperature data are from Meagher and Lager[6]; low-temperature data are from Samara and Peercy[34].

micas, pyroxenes and orthosilicates), monovalent and divalent cations appear to control the structural geometry. In these materials, which are all silicates with Mg, Fe, Ca, K or Na, electrostatic forces control most features of the structure and have a greater effect than the minor variations of covalency and electron distortions. In contrast, the RO_2 rutile-type compounds have tetravalent cations, and evidence from the bulk modulus–volume relationship indicates that bonding is more covalent than in many other oxygen-based structures. Thus, electrostatic forces may play a smaller role in determining details of the structure, compared with compounds with divalent and monovalent cations. The three factors identified by Baur and Khan[5]—nonspherical electrons, metal–metal interactions, and bond covalency—will change differently with changes in temperature versus pressure, and thus the inverse relationship fails. On the basis of this interpretation, it is predicted that covalently bonded materials are less likely to have structures that are sensitive to molar volume.

IR and Raman spectroscopy of rutile-type compounds at high temperature and high pressure may shed additional light on the unusual variation of these materials. Hara and Nicol[35], e.g. have suggested that TiO_2 is not tetragonal, but rather an intimately twinned array of orthorhombic domains, on the basis of evidence from vibrational spectroscopy and neutron diffraction. Rapid oscillations between two orientations of these domains result in a time-averaged X-ray symmetry that is tetragonal. If rutile transforms from this orthorhombic modification to a truly tetragonal form at high temperature or pressure, then the structure at high temperature may not be strictly isomorphous with the one at high pressure. Vibrational spectra of other rutile isomorphs under non-ambient conditions might help to resolve this question.

The five compounds studied, though greatly different in the electron configurations of the cations, all varied in a similar manner with changes in pressure. It is predicted, therefore, that other rutile-type compounds, including the stishovite form of SiO_2, will also compress in this way. The a axis will be approximately twice as compressible as c, and the oxygen x parameter will not vary significantly.

Acknowledgments—The authors gratefully acknowledge the contributions of T. C. Hoering, J. F. Mammone, S. K. Sharma and H. S. Yoder, Jr., who reviewed this paper. This work was supported in part by NSF Grant EAR77-23171.

REFERENCES

1. Jamieson J., In *High-Pressure Research* (Edited by M. H. Manghnani and S. Akimoto), p. 209. Academic Press, New York (1977).
2. Pistorius C. W. F. T., *Prog. Solid State Chem.* **11**, 1 (1976).
3. Liebermann R. C., *Phys. Earth Planet. Inter.* **7**, 461 (1973).
4. Liu L. G., *Science* **199**, 422 (1978).
5. Baur W. H. and Khan A. A., *Acta Cryst.* **B27**, 2133 (1971).
6. Meagher E. P. and Lager G. A., *Can. Min.* **17**, 77 (1979).
7. Hazen R. M., Finger L. W. and Yagi T., *Carnegie Instit. Washington Year Book* **77**, 841 (1978).
8. Shafer M. W., Figat R. A., Olsen B. and La Placa S. J., *IBM Research Report* RC7389. p. 10 (1978).
9. Finger L. W., Hadidiacos C. G. and Ohashi Y., *Carnegie Instit. Washington Year Book* **72**, 694 (1973).
10. Merrill L. and Bassett W. A., *Rev. Sci. Instrum.* **45**, 290 (1974).
11. Hazen R. M. and Finger L. W., *Carnegie Instit. Washington Year Book* **76**, 655 (1977).
12. Piermarini G. J., Block S., Barnett J. D. and Forman R. A., *J. Appl. Phys.* **46**, 2774 (1975).
13. Finger L. W. and Hazen R. M., *Trans. Am. Crystallogr. Assoc.* **15**, 93 (1979).
14. Hamilton W. C., *International Tables for X-ray Crystallography*, International Union of Crystallographers, Birmingham, England, Vol. 4, p. 273 (1974).
15. King H. and Finger L. W., *J. Appl. Crystallogr.* **12**, 374 (1979).
16. Finger L. W. and King H., *Am. Min.* **63**, 337 (1978).
17. Finger L. W. and Hazen R. M., *J. Appl. Phys.* **49**, 5823 (1978).
18. Zachariasen W. H., *Acta Cryst.* **A24**, 212 (1968).
19. Finger L. W. and Prince E., *Nat. Bur. Stand. (U.S.) Tech. Note* 854 (1975).
20. Cromer D. T. and Mann J. B., *Acta Cryst.* **A24**, 321 (1968).
21. Cromer D. T. and Libermann D., *J. Chem. Phys.* **53**, 1891 (1970).
22. Manghnani M., *J. Geophys. Res.* **74**, 4317 (1969).
23. Fritz I. J., *J. Phys. Chem. Solids* **35**, 817 (1974).
24. Ming L.-C. and Manghnani M. H., *J. Geophys. Res.* **84**, 4777 (1979).
25. Manghnani M. H. and Jamieson J. C., *J. Geophys. Res.* **85**, in press (1980).
26. Hazen R. M. and Finger L. W., *J. Geophys. Res.* **84**, 6723 (1979).

27. Katiyar R. S. and Krishnan R. S., *J. Indian Inst. Sci.* **51**, 121 (1969).
28. Katiyar R. S., Dawson P., Hargreave M. M. and Wilkinson G. R., *J. Phys. C* **4**, 2421 (1971).
29. Hazen R. M. and Prewitt C. T., *Am. Min.* **62**, 309 (1977).
30. Hazen R. M., *Am. Min.* **62**, 286 (1977).
31. Finger L. W. and Hazen R. M., *Am. Min.* **64**, 1002 (1979).
32. Levien L. and Prewitt C. T., *Abstracts with Programs, Geol. Soc. Am.* **11**, 465 (1979).
33. Rao K. V. K., *Am. Inst. Phys. Conf. Proc.* **17**, 219 (1974).
34. Samara G. A. and Peercy P. S., *Phys. Rev.* **B7**, 1131 (1973).
35. Hara Y. and Nicol M., *Phys. Status Solidi* **B94**, 317 (1979).
36. Robinson K., Gibbs G. V. and Ribbe P. H., *Science* **172**, 567 (1971).